EFFECT OF POINT MUTATIONS ON THE TOXICITY OF SHIGA TOXIN A1 SUBUNIT

BY

REVATI NARWANKAR

A thesis submitted to the

School of Graduate Studies

Rutgers, The State University of New Jersey

In partial fulfillment of the requirements

For the degree of

Master of Science

Graduate Program in Food Science

Written under the direction of

Nilgun E. Tumer

And approved by

_____

_____

_____

New Brunswick, New Jersey

October 2019

ABSTRACT OF THE THESIS

EFFECT OF POINT MUTATIONS ON THE TOXICITY OF SHIGA TOXIN A1 SUBUNIT

By REVATI NARWANKAR

Thesis Director:
Nilgun E. Tumer, Ph.D.

Shiga toxin (Stx)-producing *Escherichia coli* (STEC) infections can lead to life-threatening complications, including hemorrhagic colitis (HC) and hemolytic-uremic syndrome (HUS), which is the most common cause of acute renal failure in children in the United States. Previous studies have shown that STEC strains producing Stx2 are more commonly associated with HUS than those producing Stx1. Our lab has shown that the A1 subunit of Stx2 (Stx2A1) is more active than the A1 subunit of Stx1 (Stx1A1). The purpose of my study is to understand the basis for the higher toxicity of Stx2A1 by interchanging its residues with Stx1A1. Initially, the activity of wild type Stx1A1 and Stx2A1 was compared in yeast in order to establish a base line to study the effect of new mutations. We used site directed mutagenesis to exchange residues that contribute to surface charge differences between Stx1A1 and Stx2A1. Point mutations were made by interchanging Stx2A1 residues with Stx1A1 residues. If these residues contributed to the higher toxicity of Stx2A1 its toxicity would be reduced and the toxicity of Stx1A1 would be increased. The plasmids containing the mutants were transformed into yeast. The transformants were then grown in dextrose in a double overnight culture and expression was induced in

galactose. The depurination activity and cytotoxicity of the point mutants was examined at different time points post-induction. Only small differences were observed between the single point mutants and the wild type toxins in both depurination activity and cytotoxicity. In contrast, several multiple mutations increased the toxicity of Stx1A1. While double mutations did not reduce the toxicity of Stx2A1 possibly due to its higher toxicity, quadruple and quintuple mutations reduced the toxicity of Stx2.

ACKNOWLEDGEMENTS

First and foremost, I would like to thank my thesis advisor, Dr. Nilgun E. Tumer, for her continuous guidance and encouragement has been a ray of sunshine on this arduous path to competition of my thesis. Her door was always open for me whether I had a query or ran into some problems with my research and sought to help me by helping me understand the underlying principles. I would also like to greatly thank Dr. Xiao-Ping Li, Dr. Michael Pierce and Dr. Jennifer Kahn for their invaluable insight and advice through their experience in pointing me in the right direction. Special thanks to Dr. John McLaughlin for his help with the statistical analysis and for his constant belief in me to put in all my efforts to my project. Without their passionate participation and support my thesis would have lacked the finesse and expertise. I would also like to acknowledge my committee members, Dr. Donald Schaffner and Dr. Karl Matthews for their constant support and insightful guidance with my research and writing.

I would also like to express genuine appreciation for all the support, love and encourage my friends and colleagues at Rutgers University, Yijun Zhou, Stephanie Delatola, Monami Chakraborty and Manasi Date, have provided me in my years of research and study. Also, kind thanks the staff at Department of Food Science, Debbie, Laura and Raul for their help.

I would finally like to express my profound gratitude to my parents, Mahesh and Ratna Narwankar for their unfailing support, blessings and constant encouragement. It is for them that I have strived so hard to achieve this important milestone in my life. Thank you!

TABLE OF CONTENTS

LIST OF FIGURES

INTRODUCTION

Foodborne Outbreaks

The nature of food and foodborne illness has changed dramatically in the United States over the last century. The United States Department of Agriculture – Food Safety and Inspection Services (FSIS) and the Food and Drug Administration (FDA) update their rules and guidelines to keep up with these changes. For the past few decades, there has been a boom in the food industry, which, in turn, has given rise to increased instance of foodborne illness (Mead et al., 1999). As newer methods and processes are being developed to enhance the production and processing of food, there is also an increase in the likelihood for disease-causing pathogens to enter the food chain. Despite intensified efforts, foodborne illness continues to be a significant public health threat in the United States. Several trends, including large-scale production and wide distribution of food, are facilitating outbreaks of foodborne illness. These trends make it challenging to control foodborne pathogens and the frequency of infections (Nyachuba, 2010).

Several recent studies suggest that even though Norovirus remains the leading cause of foodborne illness, other enteric pathogens like *Salmonella*, *E. coli*, *Campylobacter*, *Clostridium*, and *Listeria*, still pose a significant threat to the public and are critical targets for surveillance. Shiga toxin-producing *E. coli* (STEC), *Salmonella*, *Listeria* were attributed as the common causes of hospitalizations and deaths, which were reported during outbreaks with a single person confirmed etiology (Dewey-Mattia, 2018). Out of these STEC is of significant interest because in the past two decades, the STEC has caused potential life-threatening illness.

According to CDC reports, STEC causes more than 250,000 infections per year. The infection mainly results in the development of Hemolytic Uremic Syndrome (HUS) and hemorrhagic colitis (HC). HUS is defined by acute renal injury and thrombocytopenia, which ultimately leads to kidney failure, while HC is a severe form of bloody diarrhea. A foodborne disease outbreak is defined as two or more cases of a similar illness resulting from the ingestion of a common food. It takes 2-3 weeks to confirm a STEC outbreak.

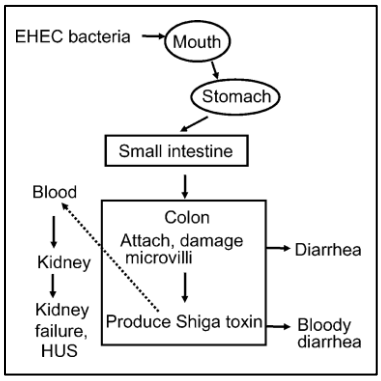

Figure 1: The development of *E. coli* infection to bloody diarrhea

As shown in Fig. 1, STEC attaches the brush border of the intestinal epithelium which combined with local and systemic effects results in the development of bloody diarrhea. Younger children, older adults, and the immuno-compromised population are generally more susceptible to the infection. Antibiotics cannot be used as a treatment for patients with STEC infections as studies have shown that antibiotics increase the risk of developing HUS by lysing the bacteria and causing the release of the toxin. Several studies as reviewed by (Kavaliauskiene et al., 2017), have studied the use of different compounds such as Chloroquine, Glucose analogs - 2-Deoxy-D-glucose and 2-Fluoro-2-deoxy-D-glucose, Retro-2 substances, manganese, inhibitors of GlcCer Synthesis PDMP and C-9, HG (Chimyl alcohol) against STEC. These compounds have been found to provide protection

against purified toxins and reduce the effects due to toxin infection. However, they have not been tested in humans due to potential side effects and more research is needed to determine if they would be safe to use in a human system. Current treatment is supportive against symptoms of HUS and HC. There are no therapeutics against STEC (Bitzan, 2009). The leading pathogenic serotype of STEC is *E. coli* O157:H7. There are hundreds of other non-O157 STEC serotypes, some of which like the O104 serotype have been found to be the cause of major Shiga outbreaks (Griffin & Tauxe, 1991; Mead & Griffin, 1998).

The first reported major STEC outbreak was the 'Jack in the box' outbreak in 1993. It was caused by the consumption of undercooked hamburgers from the restaurant chain, Jack in the box. This outbreak resulted in the death of 4 children, and over 700 people were reported sick. This outbreak resulted in significant changes in industry practices and was the turning point in food industry history due to the introduction of new food safety laws. This outbreak also led to the misconception that STEC outbreaks are usually large, multistate, and ground beef is the source of the outbreak. Further epidemiological studies have helped clear this misconception and increased the knowledge regarding STEC infections, highlighting the fact that these infections are usually small scale and, in many cases, undercooked meat, leafy vegetables, and sprouts are the source of the pathogen. Other notable outbreaks include the bean sprout outbreak in Europe in 2011, which resulted in 54 deaths and over 4000 cases of sick people. *E. coli* serotype O104 was found to be the causative agent of this outbreak highlighting new emerging *E. coli* strains other than the O157 strain which caused the earlier outbreaks (Frank et al., 2011). The multistate Chipotle outbreak in 2015, which resulted in the closure of several restaurants, and the 21-state outbreak in 2016 that caused the recall of 45 million pounds of flour by General Mills,

show how the food industry is severely affected by this pathogen (Rangel, 2005; Heiman et al., 2015; Dewey-Mattia, 2018).

E. coli and Shiga Toxin

Shiga-toxin-producing *E. coli* (STEC) was recognized as a pathogen in 1982 (Riley et al., 1983), as a critical cause of hemorrhagic colitis (HC) and Hemolytic Uremic Syndrome (HUS). *E. coli* acquired a bacteriophage that enabled it to produce toxins like *Shigella dysenteriae* Shiga toxin (Stx), named after the Japanese scientist Dr. Kiyoshi Shiga. Shiga discovered the pathogenic toxin of *Shigella dysenteriae* in 1897 during a severe epidemic of about 90,000 cases and a mortality rate of 30%.

There are almost 400 serotypes of *E. coli,* out of which at least 100 have been discovered to cause diseases in humans. This group of pathogenic *E. coli* has been categorized into six types - enterotoxigenic, enteropathogenic, enterohemorrhagic, enteroaggregative, enteroinvasive and diffuse-adhering *E. coli* (ETEC, EPEC, EHEC, EAEC, EIEC, and DAEC respectively). ETEC is characterized by adhesion to small bowel enterocytes and watery diarrhea due to the secretion of heat stable and heat-labile enterotoxins (Kaper et al., 2004). EPEC also adhere to small bowel enterocytes but cause damage to the typical microvillar structure causing inflammatory response and diarrhea. EAEC attaches to both small and large epithelia creating a thick biofilm and further increases secretion of enterotoxins and cytotoxins. EIEC attack the epithelial cells present in the colon, cause phagosome lysis and transverses the cell using nucleating actin microfilaments. DAEC induce a signal transduction effect in the small bowel enterocytes, which in turn causes the growth of long finger-like projections, that engulf bacteria. EHEC is the leading cause of many intestinal diseases in humans. Their characteristic feature is systemic absorption

leading to severe complications as seen in Stx. A study by (Konowalchuk et al., 1977) found a strain of *E. coli* that caused cytotoxic responses in an African Green Monkey cell line called Vero cell. They were named Verotoxigenic *E. coli* (VTEC) and since then have been included in the family of EHEC, together known as STEC (Alison O'Brien, 1997).

Shiga toxin 1 (Stx1) and Shiga toxin 2 (Stx2) are analogous in structure, function, and mode of action to Shiga toxin. The gene encoding for Shiga toxin 1 and Shiga toxin differ in only one amino acid, while Shiga toxin 2 shares only 58% sequence similarity with Shiga toxin 1. Stx2 is the principal causative agent in most outbreaks as it is naturally more toxic compared to Stx1. In a mouse model, the 50% lethal dose of Stx2 is 100 times lower than Stx1. However, in Vero cells, Stx1 is more toxic than Stx2.

Shiga toxins belong to ribosome inactivating proteins (RIPs). RIPs are known to inhibit protein synthesis by directly or indirectly interacting with different factors involved in the elongation step of protein synthesis. They are believed to be produced as a defense mechanism against pathogens. There are three types of RIPs found in nature. Type 1 is characterized by the presence of a single A chain, e.g., PAP (pokeweed antiviral protein), saporin, and trichosanthin. They are usually found in plants like tomato, spinach and pumpkin and crops like wheat and maize. They are 30 kDa in size and highly basic monomeric enzymes. They inhibit cell-free protein translation but are regarded as non-toxic to cells and animals. Type 2 RIPs have an A chain, and a B chain joined together by a disulfide bond, e.g., ricin, abrin, and Shiga toxin. The A chain is enzymatically active while the B chain is responsible for binding to a receptor. The sizes of the A and B chain differs in each species. Ricin has a 32 kDa A chain and a 34 kDa B chain, while Shiga toxins have a 32 kDa A chain and five copies of 7.7 kDa B chains. Type 3 RIPs require

proteolytic processing to be activated. They are synthesized as inactive precursors called as proRIPs. Type 3 RIPs are rare as compared to the other two types, and they can be isolated from maize and barley. (Damme et al., 2001; Nielsen & Boston, 2001; Peumans et al., 2001; Stirpe, 2004).

As reported (Narayanan et al., 2005), the A chain has RNA *N*-glycosidase activity, which causes the depurination of the adenine at position 4324 in the 28S rRNA of the large ribosomal subunit (Endo et al., 1988 is the first to show that Shiga toxin has N-glycosidase activity). As shown in figure 2, this adenine lies in a highly conserved 14-nucleotide region known as the α-sarcin/ricin loop (SRL). Depurination of this conserved adenine causes inhibition of elongation during translation since the elongation factors (EF) cannot bind to depurinated SRL.

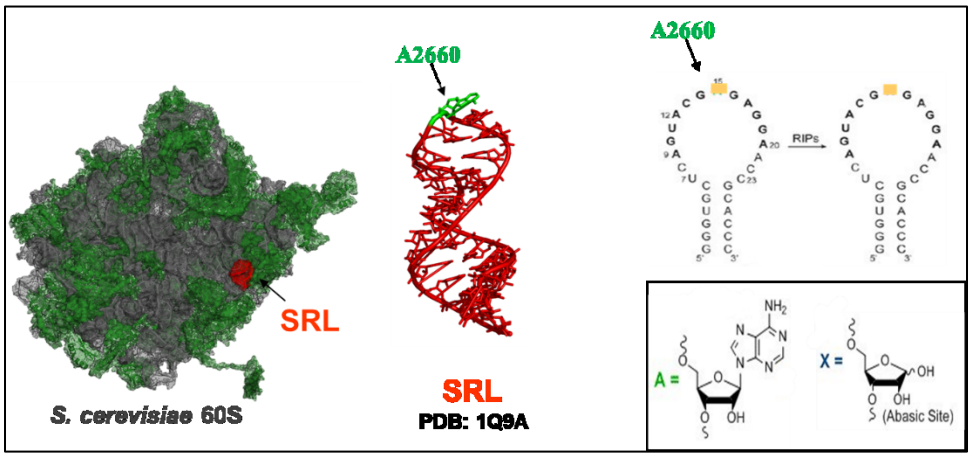

Figure 2: Depurination of adenine in the large ribosome unit in yeast.

The role of the B chain is to bind the receptor to allow uptake of RIPs into cells by endocytosis. The pentameric B subunit of Shiga toxins is responsible for binding to the Gb3 (globotriaosylceramide) receptor. The pentameric structure of the B subunit forms a

pore-like structure which nests the C- termini of the A chain. The Gb3 receptor has a total of 15 sites of the glycan component P^k trisaccharide - Galα1-4Galβ1-4Glc. Each unit in the pentamer of the B subunit has three distinct binding sites, named 1-3, which together bind to the 15 sites on Gb3. Each of these sites has a specific electron density which defines the position of the trisaccharide, of which site 2 has the highest density while site 1 has the lowest density. After endocytosis, the toxin reaches the Golgi apparatus by retrograde transport and finally the endoplasmic reticulum (ER). Here, the A1 subunit is cleaved from the A2-B5 complex due to enzymatic action of furin protease. Then the sulfide bond is reduced, and the A1 subunit undergoes retro-translocation to the cytosol where it depurinates the ribosome and initiates proinflammatory and proapoptotic signaling cascades leading to ribotoxic stress response.

In order to understand how this organism works and what are the factors involved in the development of the disease, a few years after the first Shiga outbreak in 1982, animal models were developed. Since these outbreaks had similar random sources, there was no endemic patient population to study systemic disease pathogenesis. One of the first animal models were the Gnotobiotic piglets; they had been previously used to study enteric diseases with pre-treatment. They were used in a 2002 study (Gunzer et al., 2002) where they showed a significant resemblance in the effects on GI tract and other organs. Some limitations were found in chemical and histological studies which concluded that Gnotobiotic piglets were best used for studies concerned with neurological effects as they could not simulate the full range of symptoms seen in a human system. Other systems that were developed and studied were murine (mice) models, rabbit models, and Stx challenged rodent models. However, none of these models perfectly imitated the course of the disease

as seen in humans. Although animal models provide limited information on the mechanism of the pathogenesis, they help identify biomarkers involved in the disease, which in turn help with the early diagnosis of HUS and other renal clinical syndromes.

To study the role of each subunit in the toxicity of Stx1 (VT1) and Stx2 (VT2), (Head et al., 1991) separated the A and B subunits of the holotoxin using urea and purified them using HLPC. They made hybrid toxins by interchanging the A and B subunits - VT1-A:VT2-B and VT2-A:VT1-B. It was found that the toxicity of VT1-A:VT2-B corresponded with that of VT2 and the toxicity of VT2-A:VT1-B corresponded with that of VT1, which led to the conclusion that B subunit is responsible for the toxicity of the toxin. However, they also tried producing chimeric toxins using Stx and Cholera subunits, which did not produce conclusive results due to misfolding of proteins. A study by (Russo et al., 2014) also showed similar results where subunit B was found to be the contributing factor to the higher toxicity in Vero cells. This study was also the first to show a complete set, i.e., Stx1a, Stx2a, and both the hybrids, in in-vivo and in-vitro tests. These studies highlighted the importance of the B subunit; however, the role of the A1 subunit was yet to be studied.

Due to a lack of quantitative assays that directly measure activity on ribosomes, interaction of A1 subunits with ribosomes or their catalytic activity on ribosomes has not been previously examined. Since the B subunit is required for endocytosis and retrograde trafficking, it has not been possible to study the enzymatic activity of the A1 subunits in the absence of the B subunits in vivo. Our lab pioneered yeast as a powerful model to study the catalytic activity of the A1 subunits (Chiou et al., 2011; Basu et al., 2016b; Di et al., 2017) and validated this model. We focused on the A1 subunit because 1) N-glycosidase

activity of the A1 subunit, which leads to inhibition of protein synthesis, is the lethal mechanism of Stxs; 2) the A1 subunit is known to influence potency in animal models; 3) differences in A1 subunits are responsible for differences in ribosome binding and catalytic activity; 4) we showed that the A1 subunit of Stx2 (Stx2A1) has higher affinity for ribosomes and higher catalytic activity than the A1 subunit of Stx1 (Stx1A1). Stx2A1 depurinates ribosomes and inhibits translation much more potently than Stx1A1 in human cells. These results suggested that the ribosome binding kinetics and catalytic activity of the A1 subunits, which determine the rate of depurination, may be a rate limiting step that exerts a differential influence on toxicity. Here to fill a critical gap in our understanding of the enhanced pathogenicity of Stx2 we investigated the role of the A1 subunits.

Based on previous evidence that suggested that ribosome specificity was caused due to interaction of RIPs with different ribosomal proteins, (Chiou et al., 2011) studied the expression of the A1 subunits of Stx1, Stx2 and ricin in yeast. Their results suggest that P proteins of the ribosomal stalk recruit the Stxs to the ribosome thus leading to depurination of the SRL. They also showed that Stx1 is more dependent on the ribosomal stalk than Stx2 and that both ribosome-bound and cytoplasmic pool of P1/P2 proteins play an important role in depurination. (Basu et al., 2016b) showed that the A1 subunit of Stx2 has higher affinity for ribosomes and higher catalytic activity compared to the Stx1A1 subunit. Their studies in yeast cells showed that Stx2 was ten times more toxic than Stx1 and that Stx1 showed higher expression levels at all time points. They also studied expression in mammalian cells, however the expression level was too low to detect. In the yeast model, they showed that Stx2 depurinates yeast ribosomes at significantly higher levels than Stx1 during the first 3 hours of induction in galactose. They found that a 10-fold increase in

depurination gave rise to a 40-fold increase in fold depurination in human cells. They also concluded that slight increases in depurination results in significant differences in toxicity in cells. (Basu et al., 2016a) later have shown the importance of the ribosomal P stalk protein in the binding of ribosomes, which explains the mechanism of Stx toxin and ribosome binding at a cellular level. Since, ricin and Shiga toxins share so many similarities as shown by (Sandvig, 2000), research done on ricin can be extrapolated to Shiga toxins with the hope to find similar results.

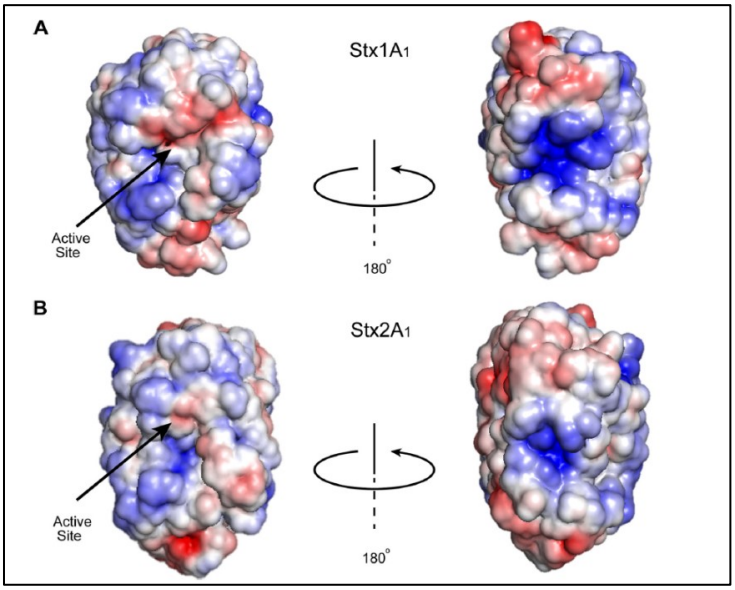

Figure 3: Surface charge distribution of (A) Shiga1A1 subunit and (B) Shiga2A1 subunit.

Comparison of the surface charge distribution of the A subunits reveals several differences in positively and negatively charged residues. As studied by (Basu et al., 2016b) and shown in figure 3, it is seen that the active site of Stx1A1 contains negatively charged residues which are absent in Stx2A1. The presence of this negatively charged zone may obstruct the interaction of the toxin with the negatively charged rRNA. After 180° rotation, it is observed that there is a large positively charged area which is more prominent in Stx1A1

compared to Stx2A1. This positively charged region present on the opposite side of the active site may allow the association with the ribosome. These differences may explain the differences in the interaction of the A1 subunits with the ribosome and the lower activity of Stx1A1 in terms of cytotoxicity and depurination compared to Stx2A1.

The purpose of this study is to understand the basis of higher toxicity of Stx2A1 by interchanging the residues that contribute to differences in the surface charge with Stx1A1. By analyzing the surface charge distribution on the toxin surface, we have selected the following residues – Q29, E60, E61, G177, and Q216 in Stx1 and E29, Y60, Y61, E177, and E215 in Stx2, to create single, double, quadruple and quintuple mutations in the A1 subunits of Stx1 and Stx2. We cloned them into the yeast vectors and studied the cell viability and ribosome depurination in yeast compared to the wild type toxins.

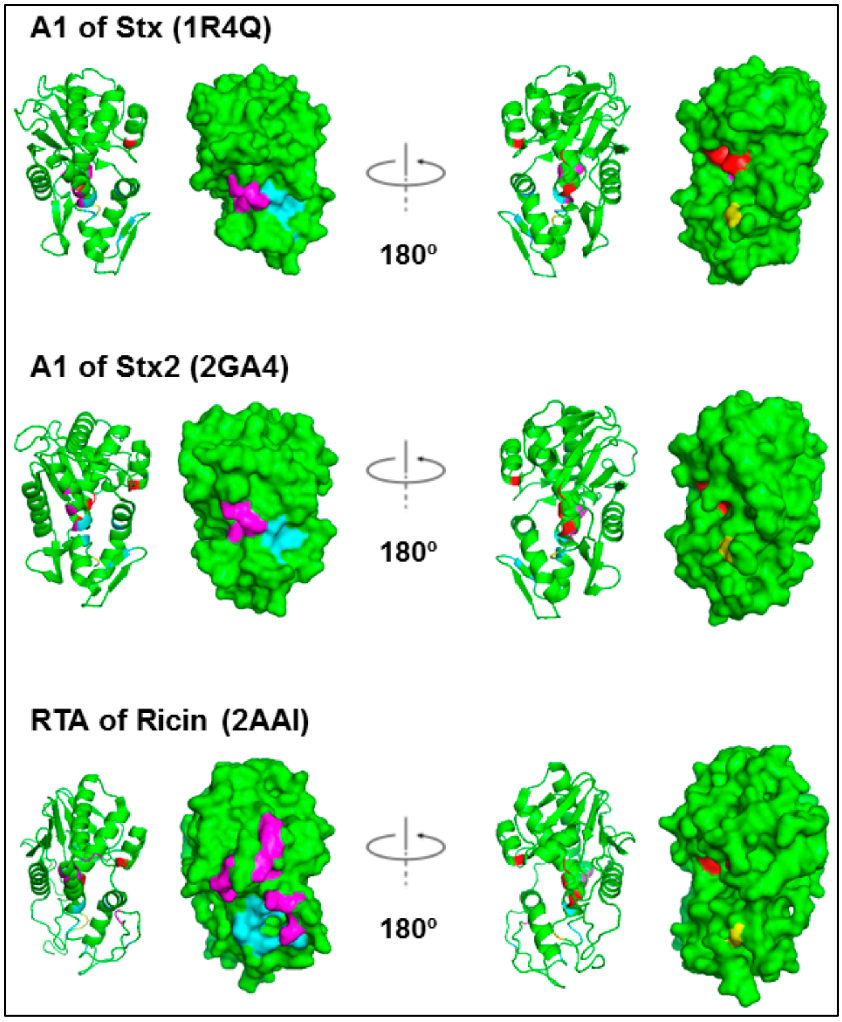

Figure 4: Structures of Stx, Stx2 and RTA shown as ribbon and surface highlight the similarities between the tree toxins.

In ricin A chain arginine 235 is critical for its interaction with the ribosomal P stalk and depurination activity (Zhou et al., 2017). The structural comparison of ricin A chain with the A1 subunit of Stx2 shows that arginine 219 and 222 in Stx2 are in the same location as Arg235 in ricin. In order to test if these arginine residues have similar binding function as ricin A chain, we created single, R219A, R222A and double, R219A/R222A mutations in Stx2A1 to determine if these residues have a significant role in the toxicity of Stx2A1.

METHODS

Site-directed Mutagenesis: Mutagenesis is a method in which a mutation is generated to study the effect on function. Mutations usually cause loss of function or alteration of function but rarely gain of function. Alterations in biological responses are studied to understand the functional role of the gene of interest. Polymerase chain reaction (PCR) is a powerful tool in genetic engineering that can be used to bring about modifications in the DNA sequence. Site-directed mutagenesis uses a pair of complementary mutagenesis primers, which allow rapid introduction of point mutations into DNA sequences and the amplification of the plasmid of interest in a single PCR cycle. In our study, we have introduced mutations into the pBlueScript vector using site-directed mutagenesis. This vector contains a His tag and V5 tag for analysis of expression and has a multi-cloning site with Xho1 and Not1 endonuclease sites that were used for cloning into the vector in our study.

Mutation-selection: We studied the surface charge distribution of Stx1 and Stx2. We chose to interchange these corresponding residues to determine their relative contribution to depurination activity. Also, comparison of the structures of RTA and Stx2A1 reveal that the R235 residue in RTA corresponds to the arginine residues at 219 and 222 on Stx2A1. To investigate whether these residues have a similar function as R235 in RTA, we created arginine to alanine single mutations - R219A, R222A and double mutation - R219A/R222A on Stx2A1.

***Design of Mutagenesis Primers*:** Primer design begins at the site of mutation in the target sequence. Once located, we extend the sequence to be at least 25- 45 base pairs in length. The melting temperature (T_m) should be greater than or equal to 78°C.

The calculation for T_m is done using the formula;

$$T_m = 81.5 + 0.41(\%GC) – 675/N - \%\ mismatch$$

For calculating Tm:

• N is the primer length in bases

• values for %GC and % mismatch are whole numbers

The desired mutation should be in the middle of the sequence. There should be a minimum of 40% GC content. The primer sequence must end in either C or G bases. This is because GC bases make stronger bonds as compared to the AT bases and ensures proper binding at the 3' end. However, higher content of GC can lead to the mis priming of the primer with the GC rich regions due to formation of primer dimers.

For the arginine to alanine mutation in wild type Stx2, we used the

Forward primer: R222A-F:

GGATGGTGTCAGAGTGGGGGCAATATCCTTTAATAATATATC

and the Reverse primer: R222A-R:

GATATATTATTAAAGGATATTGCCCCCACTCTGACACCATCC for R222A (NT1860), and

Forward primer: R219A/R222A-F:

GGATGGTGTCGCAGTGGGGGCAATATCCTTTAATAATATATC

and the Reverse primer: R219A/R222A-R:

GATATATTATTAAAGGATATTGCCCCCACTGCGACACCATCC for R219A/R222A (NT1861).

Mutagenesis PCR: We designed our PCR cycle using the cycling parameters given in the Stratagene QuikChange Site-Directed Mutagenesis protocol. We set our thermocycler for a four-stage PCR cycle which includes running at 98°C 30s, then 25 cycles of 98°C for 15-30 seconds, 62-70°C for 30 seconds, and 72°C for 4 min. This is followed by 72°C for 3-8 min and cooling to 4°C. The PCR cycle runs for 3 hours. We prepare the reaction mix with 5 µl of 5x Q5 Reaction buffer, 10 ng of dsDNA template, 0.5 µl of (10uM, 10 pmol/µl) Forward-primer, 0.5 µl of (10uM, 10 pmol/µl) Reverse-primer, 2.5 µl of dNTP mix (2mM each), then add H_2O to make up the final volume to 25µl. Finally add 0.5 µl Q5 DNA polymerase enzyme. Once the cycle completes, 5µl of the product is run on 1% agarose gel to check the quality.

Using the E.Z.N.A.® Gel Extraction Kit (Omega Bio-tek, Inc.), the product, i.e., the PCR fragment was purified. We then treat the purified product with Dpn1 enzyme, which digests the parent DNA template. The Dpn1 endonuclease is specific for methylated and hemi methylated DNA. The enzyme treatment produces a nicked vector containing the desired mutations. The Dpn1 treated sample is then cleaned using ethanol precipitation using $1/10^{th}$ volume of sodium acetate and 4 times the volume of chilled 70% ethanol. This is kept overnight at -20°C. We centrifuge the sample and air dry it to remove any trace of ethanol and then resuspend it in 50 µl ddH_2O.

The plasmid is then transformed into competent *E. coli* cells using the heat shock method. The pBlueScript vector has an amp^r gene that enables it to grow on media in the presence of ampicillin. We use LB media + Amp100 plates for the transformation. Once we get the transformed colonies, we select and grow them overnight in LB+amp media, and then using E.Z.N.A.® Plasmid DNA Mini Kit (Omega Bio-tek, Inc.), we isolate pure plasmids, and

store them at - 20℃. The mutations in the plasmid are confirmed using Sanger sequencing (Genewiz).

Cloning into the Yeast Vector: To isolate the mutated fragment, we digested the plasmids containing the desired mutated fragment in the pBlueScript vector using the restriction enzymes, Xho1 and Not1. The restriction enzyme digest resulted in a 756 bp (Stx1) and 753 bp (Stx2) fragment. We cloned the fragments into a low copy number vector, pRS415+Gal (NT1617). The NT1617 vector has an ampicillin resistance gene, a multiple cloning site and *GAL1* promoter. NT1617 is also treated with xho1/not1 restriction enzyme digestion along with the insert fragments to create sticky ends. We mix the insert and the vector in an appropriate ratio (as calculated by NEB ligation calculator) along with T4 DNA Ligase enzyme and T4 DNA Ligase Buffer to make the ligation reaction mixture. This mixture is then incubated at 16℃ overnight to ligate the fragments together.

We transformed the ligation product into competent *E. coli* cells, which produced colonies on an LB with ampicillin plate. Using these colonies, we inoculated overnight cultures in LB media and isolated pure plasmids from the culture using the plasmid isolation kit. To confirm the cloning, we treated the plasmids with restriction enzyme digestion and separated them on a DNA gel. Using Sanger sequencing, we confirmed the mutations and stored them at -20℃.

Yeast Transformation: A culture of W303 (Genotype: *MAT*a/*MAT*α {*leu2-3,112 trp1-1 can1-100 ura3-1 ade2-1 his3-11,15*} [phi^{+}]) strain yeast cells was grown overnight and then using PEG, LiOAc and single-stranded carrier DNA, we transformed the plasmid into the yeast cells by the heat shock method. We plated the transformed yeast cells onto the selective dropout media with 2% dextrose (-Ura/Dex) and incubated them at 30℃ for 48

hours. We selected colonies from the -Ura/Dex plate and streaked them on -Ura plates with 2% Dextrose (-Ura/Dex) and -Ura plates with 2% Galactose (-Ura/Gal). Galactose induces toxin expression and thus can be used to select transformed colonies. The selected colonies are then further studied in the viability and depurination assay. Three independent colonies from the transformants were examined for each mutation to ensure the consistency of results and to eliminate any outliers.

Yeast Viability Assay: We selected correctly transformed colonies in the previous step and initially grew them in -Ura/Dex media overnight. We back diluted the culture 24 hours later and grew it for another 14-16 hours. One OD cells from this culture was induced in -Ura/Gal media. Using galactose induces toxin expression in the cells. To study cell viability, we selected 1 hour, and 2 hours post-induction in galactose. At each time point, we took 0.1 OD of cells and serially diluted them to 10^{-5} dilution and plated 5 ul onto -Ura/Dex plates. We incubated the plates at 30℃ for 48 hours.

In-vivo Depurination Assay: To study the *in-vivo* depurination, we used the same colony as the yeast viability assay. We grew the culture for two nights and then induced it in -Ura/Gal media. For the depurination assay, we used 4 hours, 6 hours and 10 hours post-induction in galactose. At each time point, we took 1 OD of cells from the culture and isolated total RNA using the RNeasy Plus Mini Kit (QIAGEN). The RNA was then converted to cDNA using the High Capacity cDNA Reverse Transcription Kit (Applied Biosystems).

We used the cDNA to examine the *in-vivo* depurination by qRT-PCR analysis. We detected the depurination activity using the StepOnePlus™ Real-Time PCR system (Applied Biosystems, Grand Island, NY). To quantify the extent of depurination we used the

comparative ΔΔCT method (Pierce et al., 2011). We used two primer pairs in this method, one of which amplifies the target of interest while the other amplifies the reference amplicon which corresponds to the total RNA.

Statistical Analysis: For each yeast transformation three biological replicates were analyzed. Three transformants were chosen from a single transformation set. The depurination assay was performed with technical triplicates. Fold change in depurination was with respect to vector control. The statistical analysis was performed using the SAS software. The comparisons of the means were done, and Tukey test was used to confirm the statistical significance. The significance was determined at P value <0.05 (*), P value <0.01 (**) and P value <0.001 (***).

RESULTS

Analysis of the surface charge distribution of Stx1 and Stx2 showed that the adjacent glutamic acid residues at positions 60 and 61 on Stx1A1 are negatively charged while corresponding residues on Stx2A1 are uncharged tyrosine and glutamine residues. Stx1A1 has an uncharged glutamine residue at position 29 while Stx2A1 has a negatively charged glutamic acid residue (Figure 4). At position 177, Stx1A1 has an uncharged glycine residue whereas Stx2A1 has a negatively charged glutamic acid residue. There is an uncharged glutamine residue at position 216 on Stx1A1, while Stx2A1 has negatively charged glutamic acid residue at the corresponding site.

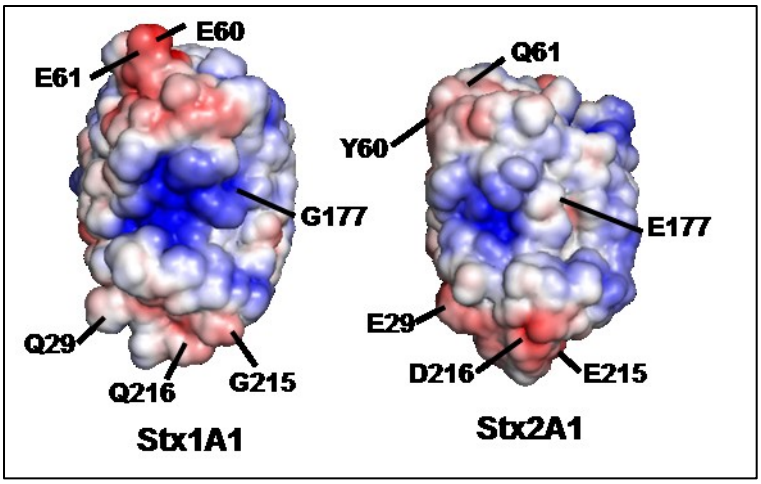

Figure 5: Crystallographic structure of Stx1A1 and Stx2A1 showing electrostatic charge distribution. {The A1 subunits of Shiga toxin and Shiga toxin 2 were modeled from the Protein Data Bank ID: 1DM0 [Shiga toxin] and 1R4P [Shiga toxin 2]) as described earlier. The surface charge difference between Stx1A1 and Stx2A1 subunit is shown (Red - negative charge; Blue - positive charge; White - neutral)}

Using site-directed mutagenesis and the specific primers, the following mutations on Stx1A1 and Stx2A1 were created: quadruple mutation - E60Y/E61Q/G177E/Q29E in Stx1, and Y60E/Q61E/E177G/E29Q in Stx2, and quintuple mutation - E60Y/E61Q/G177E/Q29E/Q216E in Stx1, and Y60E/Q61E/E177G/E29Q/E215Q in Stx2. These mutations were confirmed by sequencing.

The results obtained with the single mutants did not show significant differences, which led to the hypothesis that more than one mutation is needed to enhance the toxicity of Stx1A1 and to reduce the toxicity of Stx2A1. We present and discuss the results of double, quadruple and quintuple mutations in Stx1A1 and Stx2A1, and arginine to alanine mutations in Stx2A1.

Effect of mutations on the toxicity of Stx1A1:

Since Stx1A1 has lower toxicity in yeast compared to Stx2A1, we anticipated that the mutation would increase the toxicity and depurination activity of Stx1A1 compared to the wild type Stx1A1. Surface charge analysis revealed that Stx1A1 has negatively charged E60 and E61 residues, which are missing in Stx2A1. It also has G177 residue which corresponds to negatively charged E177 residue in Stx2A1 and that Stx2A1 has negatively charged E216 and E215 residues which are missing in Stx1A1.

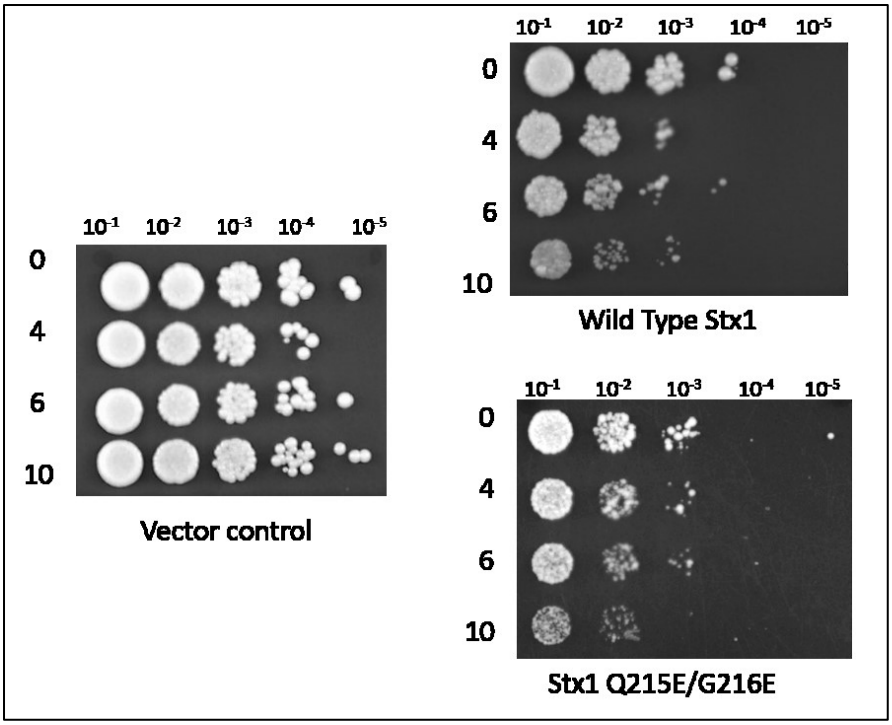

Figure 6: Viability assay of G215E/Q216E mutant in Stx1A1 subunit at 0, 4, 6 and 10 hours post-induction. The viability test was repeated with three colonies and one representative experiment is shown.

In the double mutant study, as seen in Figure 6, we can deduce that the mutant becomes slightly toxic as compared to wild type. This is indicated by the reduction in the density of cells from the 10^{-2} dilutions to the 10^{-5} dilutions at 4-, 6-, and 10- hour timepoints.

We performed the depurination assay, and it is observed (Figure 7) that G215E/Q216E mutant in Stx1A1 results in no change in the depurination activity at 0-hour and 2-hour post-induction time point. There is an increase in toxicity indicated by the increase in fold depurination as compared to the wild type Stx1. There is a significant increase in the fold depurination level of the mutant at 1-hour post-induction. It is observed that there is an approximately 1.6 times increase in the depurination activity.

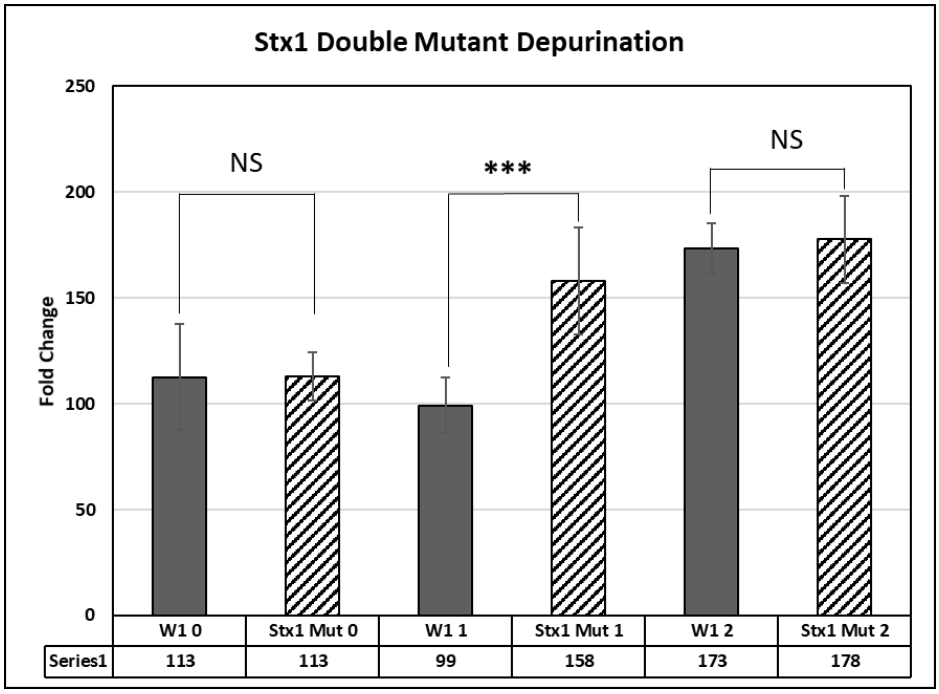

Figure 7: Change in fold depurination level of the G215E/Q216E mutant in Stx1A1 as compared with the wild type Stx1 at 0, 1, and 2 hours post-induction. The error bars represent S.E n=3. The means were significant at *P<0.05; **P<0.01;***P<0.001.

We hypothesized that if double mutation can result a small increase in the depurination activity, making more than two mutations by exchanging residues with Stx2A1, would further increase the toxicity of Stx1A1. In our study, we made quadruple - E60Y/E61Q/G177E/Q29E and quintuple mutations - E60Y/E61Q/G177E/Q29E/Q216E. Here, we present the results of the viability and *in-vivo* depurination assay for the multiple mutants.

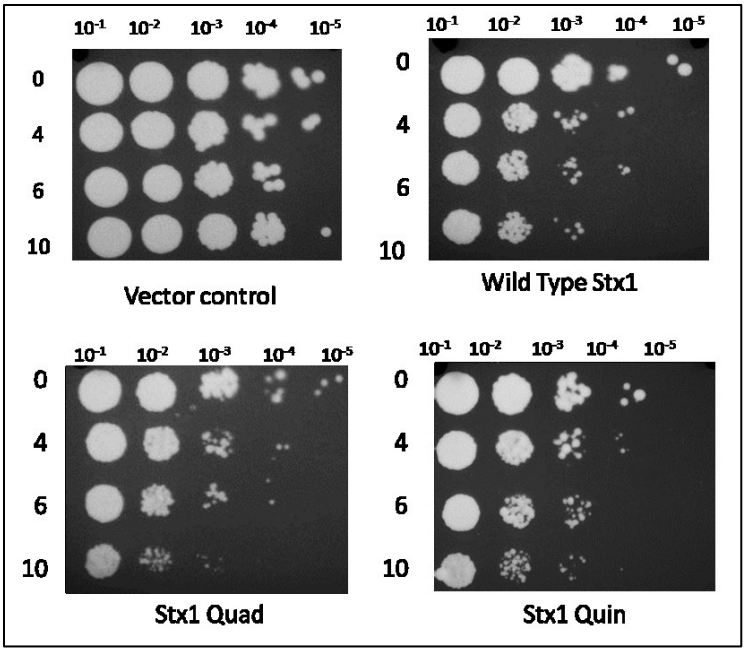

Figure 8: Viability assay of E60Y/E61Q/G177E/Q29E (Quadruple) and E60Y/E61Q/G177E/Q29E/Q216E (Quintuple) mutations in Stx1A1 subunit at 0, 4, 6 and 10 hours post-induction. The viability test was repeated with three colonies and one representative experiment is shown.

Figure 8 shows that the wild type has higher growth of cells due to lower toxicity. The quadruple mutation has increased the toxicity to a small extent as is evident by the decrease in cell density at the 10^{-2} and 10^{-3} dilutions of the 10-hour time point. Cell growth in the quadruple mutant is visibly lower than that for the quintuple mutant which suggests that the addition of the Q216 mutation in the quintuple mutant did not increase the toxicity as expected but may have reduced the toxicity resulting in a higher growth of cells.

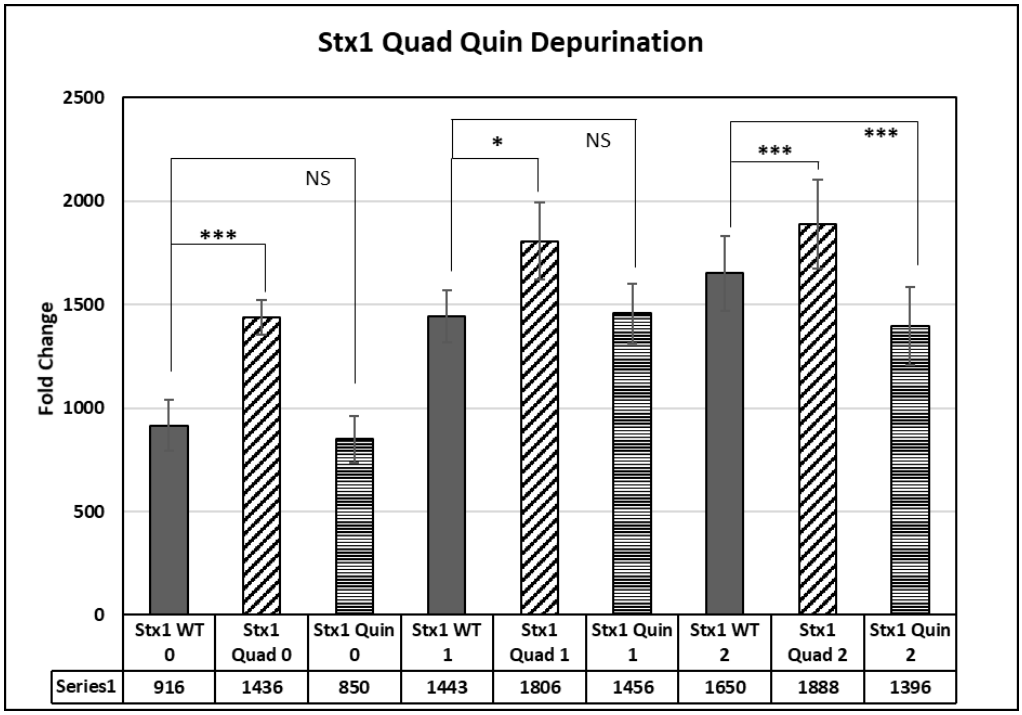

Figure 9 : Fold change in the depurination activity of quadruple mutant - E60Y/E61Q/G177E/Q29E, and the quintuple mutant - E60Y/E61Q/G177E/Q29E/Q216E in Stx1A1. The error bars represent S.E n=3. The means were significant at *P<0.05; **P<0.01;***P<0.001.

In Figure 9, we can observe the change in the depurination activity due to the quadruple- E60Y/E61Q/G177E/Q29E and the quintuple mutations- E60Y/E61Q/G177E/Q29E/Q216E. The study reveals that overall the quadruple mutation seems to have caused a more significant increase in the depurination activity as compared to the quintuple mutation. This correlates with our study of the yeast cell viability and indicates that the Q216E mutation in Stx1A1 subunit may be unstable or may have a negative effect causing it to further decrease the toxicity than the wild type.

Effect of mutations on the toxicity of Stx2A1:

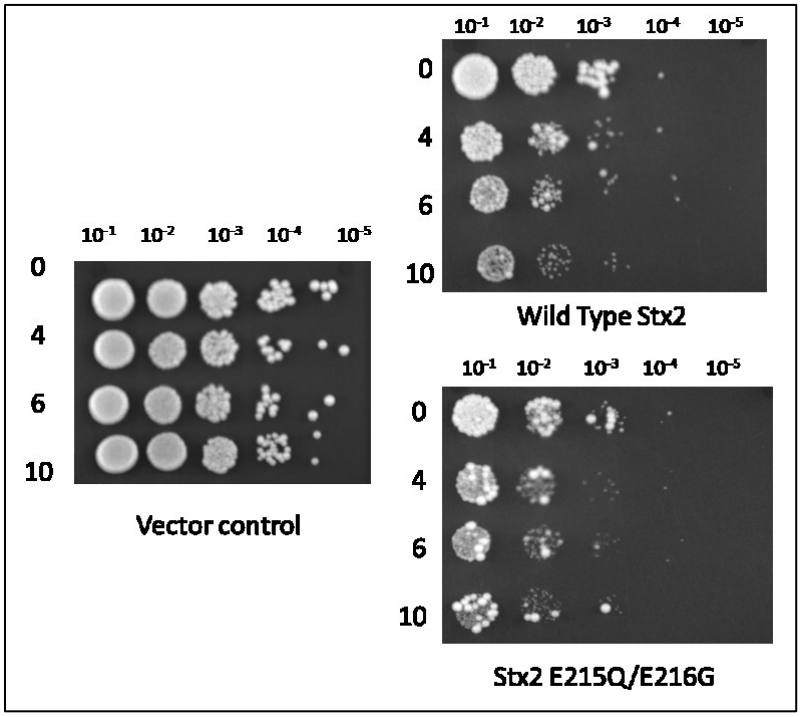

Figure 10: Viability assay of E215G/E216Q mutation in Stx2A1 subunit at 0, 4, 6 and 10 hours post-induction. The viability test was repeated with three colonies and one representative experiment is shown.

Figure 10 shows that there is growth of bigger cells likely suppressor cells among the smaller ones which may outgrow the primary cells, thus giving false results. Lower growth of non-suppressor cells was observed in the 10^{-3} dilution, which indicates slightly increased toxicity. We also observe that there is lower density of cells at the 6- and 10-hour time point which may indicate that as time progresses the toxicity of the mutant seems to increase. Even though there are double mutations, it is seen that the toxicity of the Stx2A1 subunit remains unaltered or seems to increase.

Analysis of the in-vivo depurination assay (Figure 11) shows no significant change in the toxicity of the mutant as compared to the wild type Stx2A1 during the first hour of induction on galactose. At 2 hours after induction, there is a 2-fold increase in the

depurination activity. This correlates with the viability assay and again highlights the fact that the double mutation causes an increase in the toxicity with time.

Since the double mutations do not seem to reduce the toxicity of Stx2A1 to a significant level, we infer that interchanging more residues should have a higher effect due to their cumulative effect of reducing the negative charge on the surface of the toxin.

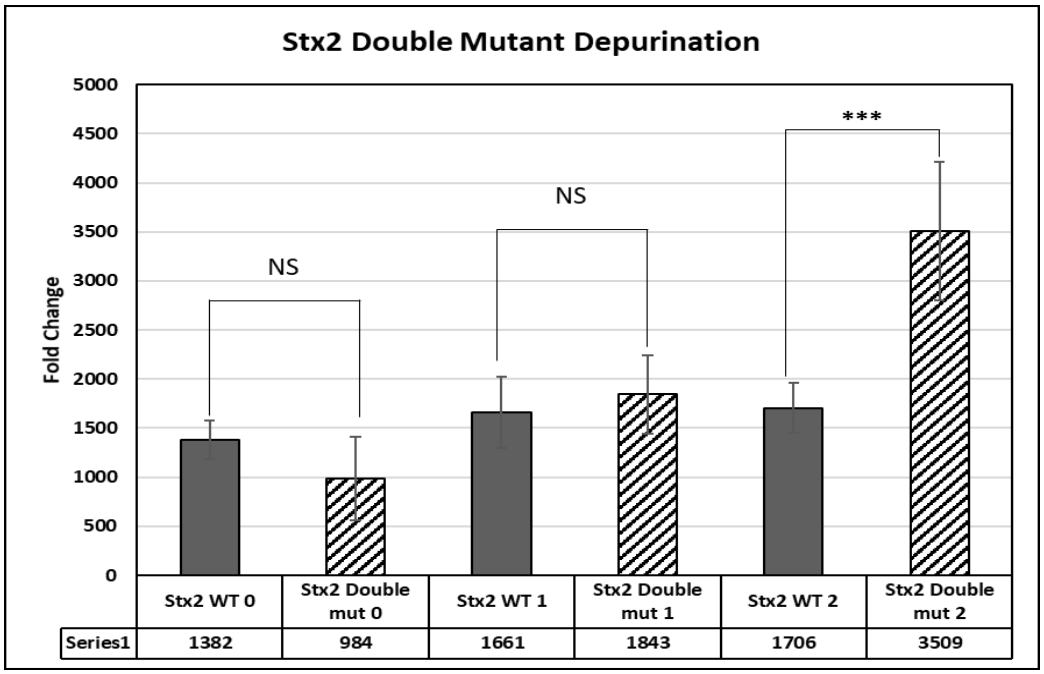

Figure 11: Change in fold depurination level of the E215G/E216Q mutant in Stx2A1 as compared with the wild type Stx1 at 0, 1, and 2 hours post-induction. The error bars represent S.E n=3. The means were significant at *P<0.05; **P<0.01;***P<0.001.

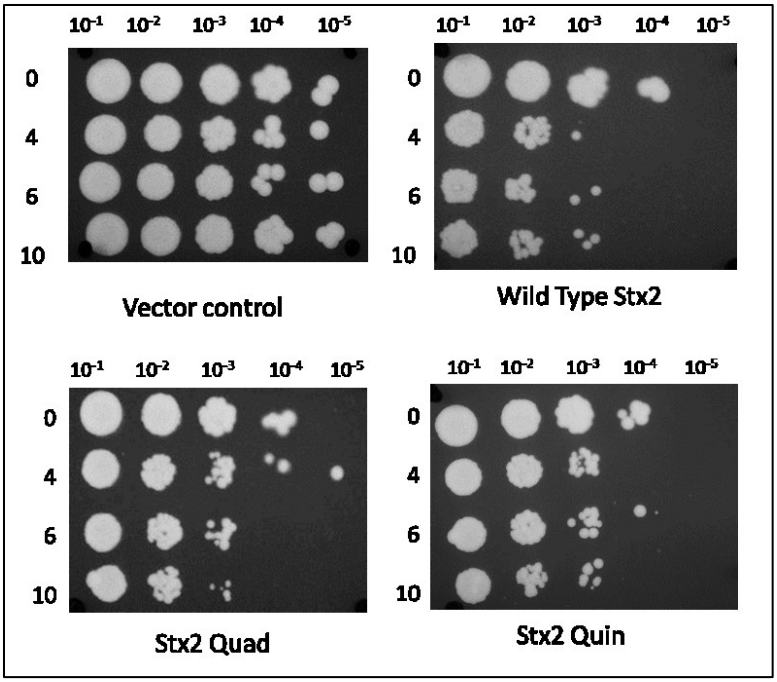

Figure 12: Viability assay of Y60E/Q61E/E177G/E29Q (Quadruple) Y60E/Q61E/E177G/E29Q/E215Q (Quintuple) mutant in Stx2A1 subunit at 0, 4, 6 and 10 hours post-induction. The viability test was repeated with three colonies and one representative experiment is shown.

As seen in Figure 12, there is a slight increase in the viability of both mutants indicating that there has been a small decrease in the toxicity of the mutants at the 4-hour time point as compared to the wild type. By the 10-hour time point it is observed that the effect of the mutations decreases, and there is less reduction in toxicity.

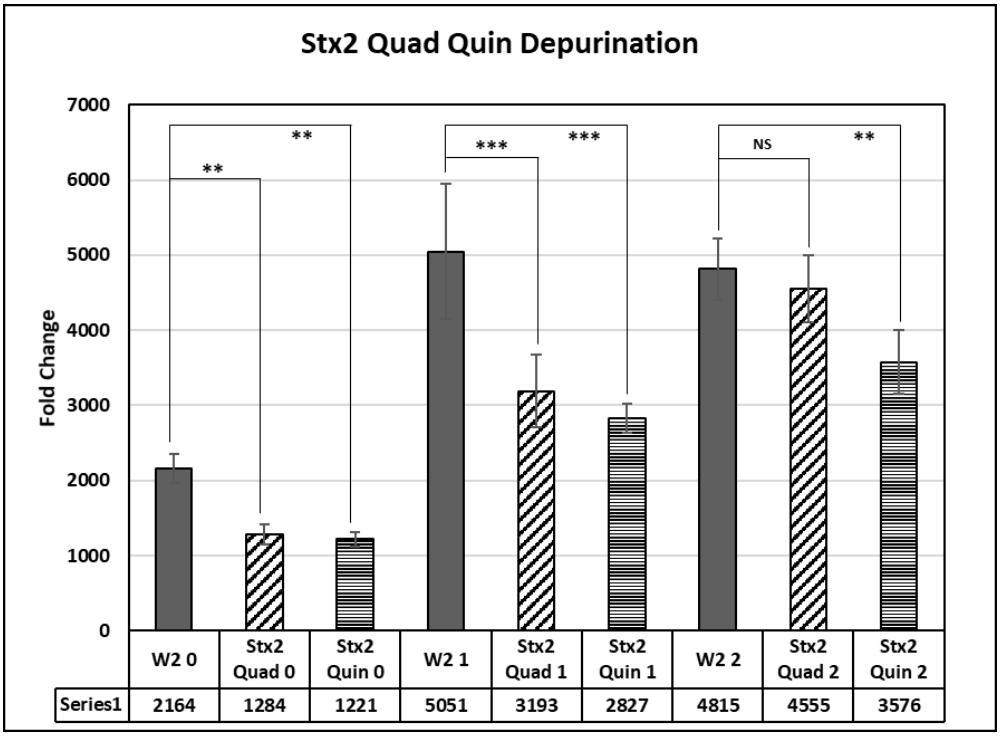

Figure 13: Fold change in the depurination activity Y60E/Q61E/E177G/E29Q (Quadruple) Y60E/Q61E/E177G/E29Q/E215Q (Quintuple) mutant in Stx2A1 subunit as compared with the wild type Stx1 at 0,1,and 2 hours post-induction. The error bars represent S.E n=3. The means were significant at (*P<0.05; **P<0.01;***P<0.001).

The depurination data (Figure 13) shows that the quintuple - Y60E/Q61E/E177G/E29Q/E215Q mutant reduces the toxicity of Stx2A1. At the 0-hour, both the quadruple mutant - Y60E/Q61E/E177G/E29Q, and the quintuple mutant result in a significant decrease in the depurination activity as compared to the wild type. However, at the 1-hour time point, both mutations cause a significant decrease in the depurination activity. At 2-hour time point, the quadruple mutation causes a non-significant decrease in the fold depurination while the quintuple mutation causes a significant decrease in the depurination activity. The results mirror those of the viability assay and show that the

replacement of five different electrostatic residues is needed to reduce the depurination activity and toxicity of Stx2A1.

Effect of Arginine to Alanine Mutations:

In a previous study by (Zhou et al., 2017), R235 was a critical residue in the ribosome binding mechanism of ricin A chain (RTA). Mutations in R235 residue and its surrounding residues showed that even though R235 itself has lower depurination activity, together with its surrounding residues they contribute to fast electrostatic interactions with the ribosome. The results of the investigation of arginine to alanine single mutations - R219A, R222A and double mutation - R219A/R222A on Stx2A1 are presented here.

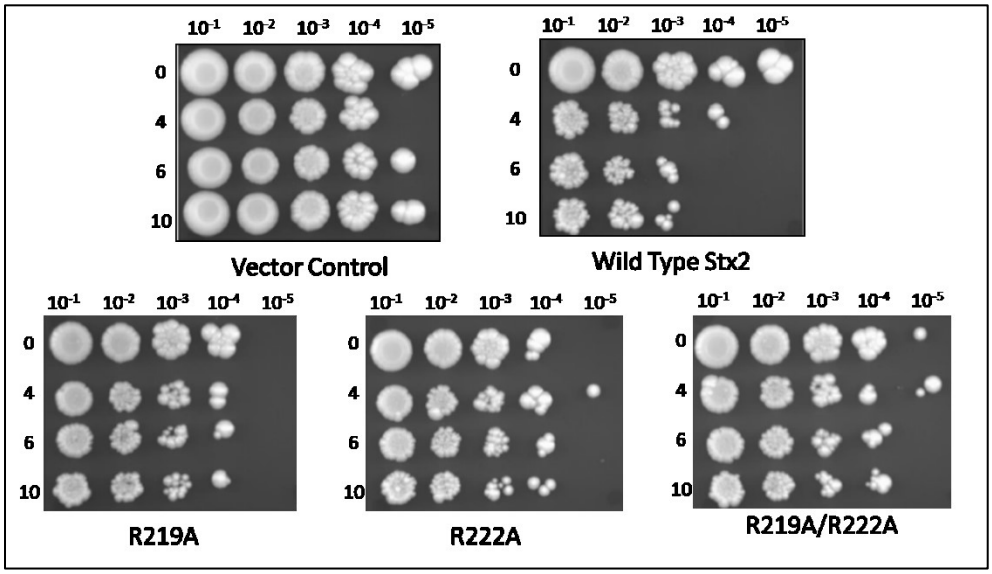

Figure 14: Viability assay of arginine to alanine mutations, R219A, R222A and R219A/R222A in Stx2A1 at 0, 4, 6, and 10 hours post-induction. The viability test was repeated with three colonies and one representative experiment is shown.

Figure 14 shows an overall decrease in toxicity of the arginine mutants depicted by increased cell growth as compared to the WT Stx2. In the single mutants R219A and R222A, there is an increase in the number of viable cells at the 6- and 10- hour time points

for the 10^{-4} and 10^{-5} dilutions as compared to the wild type. The double mutant shows a higher reduction in the toxicity with increased cell growth at all time points.

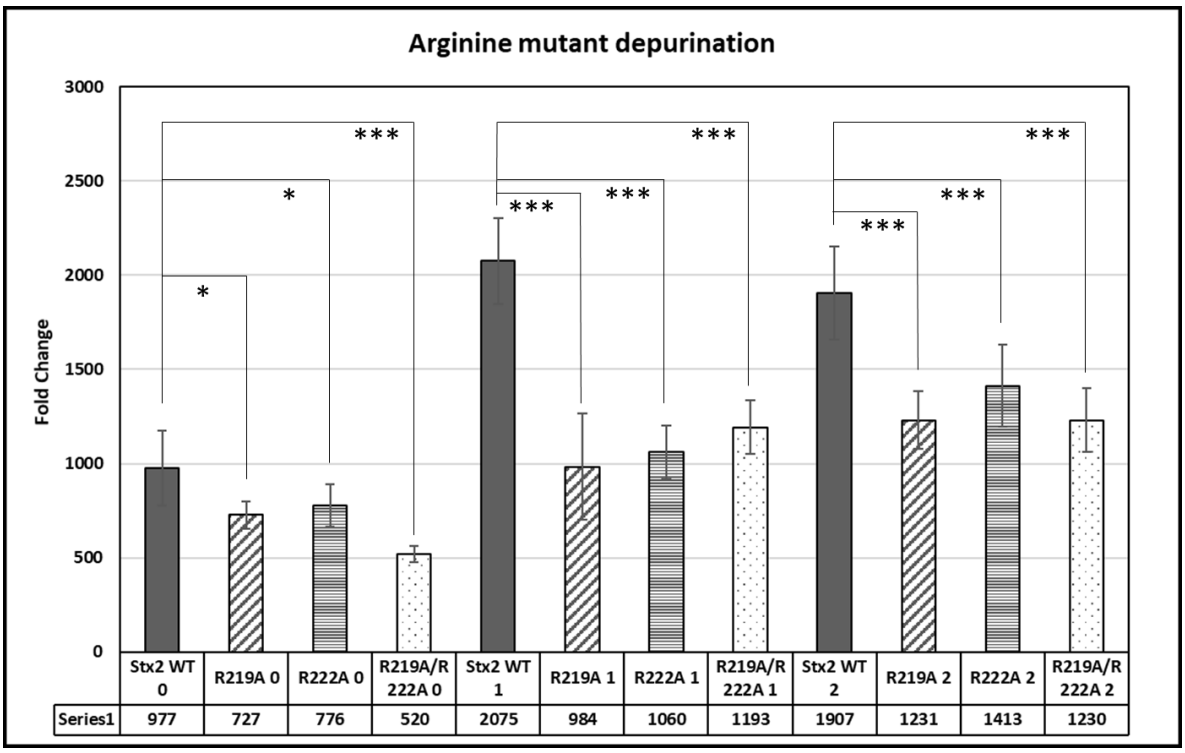

Figure 15: Fold change in the depurination activity of R219A, R222A and R219A/R222A mutant in Stx2A1 subunit as compared with the wild type Stx2 at 0, 1, and 2 hours post-induction. The error bars represent S.E n=3. The means were studied at significance values (*P<0.05; **P<0.01;***P<0.001).

Our analysis reveals (Figure 15) a considerable reduction in the depurination activity across all mutants as compared to the WT Stx2A1. In addition, the depurination activity of the WT Stx2A1 increases two-fold after induction in galactose media. At 0-hour, the double mutant has a higher reduction in the depurination activity than the single mutant. At 1-hour post-induction, the single mutants have a two-fold reduction in activity whereas the double mutant has less than two-fold reduction. Furthermore, at the 2-hour time point, all mutants

show an increase in activity, however, the reduction in toxicity is significantly higher for the mutants as compared to the wild type.

DISCUSSION

Although the structures of Stx and Stx2 are similar, the sequence divergence between Stx2A1 and Stx1A1 has some influence on the structure (Basu et al., 2016b). Previous studies have shown that the A1 subunit of Stx2 is catalytically more active and depurinates both naked RNA as well as ribosomes at a higher rate than the A1 subunit of Stx1A1. Stx2A1 also has a higher affinity for the ribosome than Stx1A1 (Basu et al., 2016b). We previously showed that the conserved active site (E167 and R170) and the ribosome stalk binding site residues (R172, R176, R179) do not contribute to the higher ribosome binding and depurination activity of Stx2. There are other residues that differ in surface exposure which may influence the function of the A1 subunits differently and may be responsible for the higher catalytic activity of Stx2A1 compared to Stx1A1.

In our previous study, we interchanged E60 and E61 in Stx1A1 with Y60 and Q61 in Stx2A1 to examine the effect of these mutations on depurination activity and toxicity of Stx1A1 and Stx2A1 by expressing each mutant in yeast and analyzing their viability and depurination activity. These mutants were toxic, and we were unable to detect any significant difference in viability between the E60Y/E61Q in Stx1A1 and Y60E/Q61E in Stx2A1 and the corresponding wild type A1 subunits. However, when we measured their depurination level, there is a significant increase in the depurination of E60Y/E61Q in Stx1A1 and a significant decrease in depurination of Y60E/Q61E in Stx2A1 in comparison to their WT (Basu et al., unpublished data). Since depurination is an upstream event in comparison to cell death and viability and is a more quantitative and sensitive assay in comparison to the viability assay, it allowed us to observe the effects of surface charge modifications in the activity of Stx1A1 and Stx2A1. The negatively charged knob on

Stx1A1 played a role in the depurination activity of Stx1A1, probably by influencing the binding of the Stx1A1 toxin to the negatively charged ribosome and the sarcin/ricin loop (SRL). By converting the glutamic acids at position 60 and 61 in Stx1A1 to neutral Y and Q, the negatively charged ribosome becomes more accessible. This is further corroborated by the fact that the depurination level of Stx2A1 is reduced when the neutral Y and Q at positions 60 and 61 is changed to the negative glutamic acids. The Stx2A1 mutant is now repelled by the negatively charged ribosome and therefore shows lower depurination. These results indicate that electrostatic interaction of the toxins with the ribosome is critical and showed that the residues that are away from the active site and ribosome stalk binding site and are not conserved between Stx1A1 and Stx2A1 play a vital role in viability and depurination activity. However, by mutating only 2 residues we observed small changes. In order to determine if mutating additional residues that contribute to surface charge differences will cause larger difference, we mutated other residues and combined those mutations. Our results show that simultaneously altering the electrostatic charge distribution significantly increases the depurination activity and toxicity of Stx1A1 and reduces the depurination activity and toxicity of Stx2A1.

According to previous studies by (Li et al., 2009, 2010, 2013), the toxins concentrate around the ribosome surface by electrostatic interactions before they reach the P protein stalk. These interactions involve residues that are positively charged and hence we aim to find residues that contribute to these electrostatic interactions. Study of the surface residues revealed that Stx1A1 has a negatively charged knob which is absent in Stx2A1, and that the mutations that exchanged these residues increased the depurination activity of Stx1A1 and decreased the depurination activity of Stx2A1 (Basu, 2016). It is also observed that

Stx2A1 has negatively charged D216 and E215 residues which are missing in Stx1A1. This led us to create double mutations G215E/Q216E in Stx1 and E215G/E216Q in Stx2 by exchanging the residues at positions 215 and 216. These mutants were then tested for their cytotoxicity and depurination activity as compared to the WT. Yeast viability assays did not show any significant differences; however, there was a slight increase in the toxicity of the Stx1A1 mutant. The depurination assay showed a significant increase in the toxicity of Stx1A1 at 1-hour post-induction. These results indicate that since these residues are away from the active site the negative charge may not cause any obstruction in the ribosome binding. Instead, the presence of glutamic acid at these positions assists ribosome binding and increases the depurination activity of Stx1A1. In contrast, in Stx2A1 the loss of the two negatively charged residues significantly increases the depurination activity at 2-hours post-induction. This could be possibly because loss of the negative charge increases the interaction with the negatively charged ribosome and hence causes a higher level of depurination by Stx2A1.

Since Stx2A1 has a higher activity, the negatively charged residues away from the active site do not have any effect on the ribosome binding due to their negative charge. To investigate if multiple mutations have a cumulative effect on the toxicity of Stx1A1 and Stx2A1 toxins, we interchanged residues at 60, and 61 position like the earlier study (Basu, 2016) along with residues at position 29, 177 and 215. This resulted in the quadruple mutant, E60Y/E61Q/G177E/Q29E, in Stx1A1 and Y60E/Q61E/E177G/E29Q in Stx2A1, and the quintuple mutant, E60Y/E61Q/G177E/Q29E/Q216E, in Stx1A1 and Y60E/Q61E/E177G/E29Q/E215Q in Stx2A1.

The viability and depurination results indicate that the addition of the negative charge at position 216 seems to reduce the toxicity of Stx1A1 and hence this mutant depurinates at a lower level than the WT Stx1A1. In the case of Stx2A1, the mutations seem to have an overall reducing effect on the depurination activity of the mutants. However, it is interesting to observe that the quintuple mutant significantly reduces the toxicity more than the quadruple mutant at 2- hours post-induction. This indicates that the loss of negatively charged residues at positions 60 and 61 combined with the loss of the negative charge at position 215 has a higher effect and reduces the depurination activity of Stx2A1 by approximately 1.3 times. Although the fold reduction in depurination seems low, this reduction is amplified in cells by ribotoxic signaling and thus it has been shown that small differences in depurination activity could result in much bigger differences in toxicity in cells and in animal models.

Another study by (Zhou et al., 2017), highlighted the importance of arginine 235 in the toxicity of RTA. It was shown that this residue present at the interface of the A and B subunits of ricin has a significant role in the depurination activity and ribosome binding. It was also discovered that when R235 is mutated with its neighboring residues it causes a further reduction in activity. Comparison of the sequence of Stx2A1 and RTA showed that Stx2A1 has R219 and R222 at the same corresponding position as R235 in RTA. We hypothesized that mutation of these residues may have the same effect in Stx2A1 as in RTA. We created the mutations by replacing the arginine residues with alanine residues. Arginine to alanine mutations reduce the positive charge without adding any other charge since alanine is a neutral residue. These mutations may affect ribosome binding in the non-conserved regions between Stx1A1 and Stx2A1 while maintaining the interaction with the

P stalk, which in turn would indicate if these residues are involved in the non-stalk specific interactions. This reduction in the positive charge would interfere with the binding mechanism to the ribosome and would reduce the toxicity. To test this hypothesis, we tested the mutants in yeast by growing them on galactose to induce toxin production. The toxicity began to decrease at 4-hours post-induction and continued to decrease up to 10-hours with the double mutant being more effective. To confirm this reduction in cytotoxicity, we determined the mutants' depurination activity. While there is an overall significant decrease in the depurination activity it is noted that the double mutant caused a higher reduction than either of the single mutants before the induction. Once induced, there were slight differences in the activity, but the single mutation at position 219 and the double mutation seemed to cause a higher reduction. This study demonstrated that the reduction in the positive charge on the surface of the Stx2A1 subunit reduced the depurination activity and the toxicity possibly by affecting the interaction with the ribosome.

This study and its results are significant because they help us understand how we can reduce the toxicity of Stx2A1. Where earlier studies have shown that the B subunit does not account for the cytotoxicity entirely, we have shown that the A1 subunit has a prominent role in the increased cytotoxicity of Stx2. Our results identify residues outside the active site that are critical for the depurination activity and demonstrate that residues that contribute to surface charge differences play a major role in the higher depurination activity and toxicity of Stx2A1 compared to Stx1A1.

REFERENCES

1. Mead, P. S., Slutsker, L., Dietz, V., McCaig, L. F., Bresee, J. S., Shapiro, C., … Tauxe, R. V. (1999). Food-related illness and death in the United States. *Emerging Infectious Diseases*, *5*(5), 607–625.

2. Nyachuba, D. G. (2010). Foodborne illness: Is it on the rise? Nutrition Reviews©, Vol. 68, No. 5. *Nutrition Reviews*, *68*(5), 257–269. https://doi.org/10.1111/j.1753-4887.2010.00286.x

3. Dewey-Mattia, D. (2018). Surveillance for Foodborne Disease Outbreaks — United States, 2009–2015. *MMWR. Surveillance Summaries*, *67*. https://doi.org/10.15585/mmwr.ss6710a1

4. Kavaliauskiene, S., Dyve Lingelem, A., Skotland, T., & Sandvig, K. (2017). Protection against Shiga Toxins. *Toxins*, *9*(2), 44. https://doi.org/10.3390/toxins9020044

5. Bitzan, M. (2009). Treatment options for HUS secondary to *Escherichia coli* O157:H7. *Kidney International*, *75*, S62–S66. https://doi.org/10.1038/ki.2008.624

6. Griffin, P. M., & Tauxe, R. V. (1991). *The Epidemiology of Infections Caused by Escherichia coli O157:H7, Other Enterohemorrhagic £. coli, and the Associated Hemolytic Uremic Syndrome*. *13*, 39.

7. Mead, P. S., & Griffin, P. M. (1998). *Escherichia coli* O157:H7. *The Lancet*, *352*(9135), 1207–1212. https://doi.org/10.1016/S0140-6736(98)01267-7

8. Rangel, J. M. (2005). *Epidemiology of Escherichia coli O157:H7 Outbreaks, United States, 1982–2002*. *11*(4). https://doi.org/10.3201/eid1104.040739

9. Heiman, K. E., Mody, R. K., Johnson, S. D., Griffin, P. M., & Gould, L. H. (2015). *Escherichia coli* O157 Outbreaks in the United States, 2003–2012. *Emerging Infectious Diseases*, *21*(8), 1293–1301. https://doi.org/10.3201/eid2108.141364

10. Kaper, J. B., Nataro, J. P., & Mobley, H. L. T. (2004). Pathogenic *Escherichia coli*. *Nature Reviews Microbiology*, *2*(2), 123. https://doi.org/10.1038/nrmicro818

11. Konowalchuk, J., Speirs, J. I., & Stavric, S. (1977). Vero response to a cytotoxin of *Escherichia coli*. *Infection and Immunity*, *18*(3), 775–779.

12. Alison O'Brien. (1997). *Third International Symposium of Shiga Toxin (Verocytotoxin) - Producing Escherichia coli Infections (VTEC '97).* Retrieved from Lois Joy Galler Foundation for Hemolytic Uremic Syndrome Inc., Melville NY website: https://apps.dtic.mil/docs/citations/ADA328167

13. Damme, E. J. M. V., Hao, Q., Chen, Y., Barre, A., Vandenbussche, F., Desmyter, S., … Peumans, W. J. (2001). Ribosome-Inactivating Proteins: A Family of Plant Proteins That Do More Than Inactivate Ribosomes. *Critical Reviews in Plant Sciences*, *20*(5), 395–465. https://doi.org/10.1080/07352689.2001.10131826

14. Nielsen, K., & Boston, R. S. (2001). RIBOSOME-INACTIVATING PROTEINS: A Plant Perspective. *Annual Review of Plant Physiology and Plant Molecular Biology*, *52*(1), 785–816. https://doi.org/10.1146/annurev.arplant.52.1.785

15. Peumans, W. J., Hao, Q., & Van Damme, E. J. M. (2001). Ribosome-inactivating proteins from plants: More than RNA N-glycosidases? *The FASEB Journal*, *15*(9), 1493–1506. https://doi.org/10.1096/fj.00-0751rev

16. Narayanan, S., Surendranath, K., Bora, N., Surolia, A., & Karande, A. A. (2005). Ribosome inactivating proteins and apoptosis. *FEBS Letters*, *579*(6), 1324–1331. https://doi.org/10.1016/j.febslet.2005.01.038

17. Endo, Y., Tsurugi, K., Yutsudo, T., Takeda, Y., Ogasawara, T., & Igarashi, K. (1988). Site of action of a Vero toxin (VT2) from *Escherichia coli* O157:H7 and of Shiga toxin on eukaryotic ribosomes. *European Journal of Biochemistry*, *171*(1–2), 45–50. https://doi.org/10.1111/j.1432-1033.1988.tb13756.x

18. Gunzer, F., Hennig-Pauka, I., Waldmann, K.-H., Sandhoff, R., Gröne, H.-J., Kreipe, H.-H., … Mengel, M. (2002). Gnotobiotic Piglets Develop Thrombotic Microangiopathy After Oral Infection with Enterohemorrhagic *Escherichia coli*. *American Journal of Clinical Pathology*, *118*(3), 364–375. https://doi.org/10.1309/UMW9-D06Q-M94Q-JGH2

19. Head, S. C., Karmali, M. A., & Lingwood, C. A. (1991). Preparation of VT1 and VT2 hybrid toxins from their purified dissociated subunits. Evidence for B subunit modulation of a subunit function. *The Journal of Biological Chemistry*, *266*(6), 3617–3621.

20. Russo, L. M., Melton-Celsa, A. R., Smith, M. J., & O'Brien, A. D. (2014). Comparisons of Native Shiga Toxins (Stxs) Type 1 and 2 with Chimeric Toxins Indicate that the Source of the Binding Subunit Dictates Degree of Toxicity. *PLOS ONE*, *9*(3), e93463. https://doi.org/10.1371/journal.pone.0093463

21. Chiou, J.-C., Li, X.-P., Remacha, M., Ballesta, J. P. G., & Tumer, N. E. (2011). Shiga toxin 1 is more dependent on the P proteins of the ribosomal stalk for depurination activity than Shiga toxin 2. *The International Journal of Biochemistry & Cell Biology*, *43*(12), 1792–1801. https://doi.org/10.1016/j.biocel.2011.08.018

22. Basu, D., Li, X.-P., Kahn, J. N., May, K. L., Kahn, P. C., & Tumer, N. E. (2016). The A1 Subunit of Shiga Toxin 2 Has Higher Affinity for Ribosomes and Higher

Catalytic Activity than the A1 Subunit of Shiga Toxin 1. *Infection and Immunity*, *84*(1), 149–161. https://doi.org/10.1128/IAI.00994-15

23. Di, R., Vakkalanka, M. S., Onumpai, C., Chau, H. K., White, A., Rastall, R. A., … Hotchkiss, A. T. (2017). Pectic oligosaccharide structure-function relationships: Prebiotics, inhibitors of *Escherichia coli* O157:H7 adhesion and reduction of Shiga toxin cytotoxicity in HT29 cells. *Food Chemistry*, *227*, 245–254. https://doi.org/10.1016/j.foodchem.2017.01.100

24. Sandvig, K. (2000). REVIEW: Entry of ricin and Shiga toxin into cells: molecular mechanisms and medical perspectives. *The EMBO Journal*, *19*(22), 5943–5950. https://doi.org/10.1093/emboj/19.22.5943

25. Zhou, Y., Xiao-Ping Li, Brian Y. Chen, & Nilgun E. Tumer. (2017). *Ricin uses arginine 235 as an anchor residue to bind to P-proteins of the ribosomal stalk*. https://doi.org/10.1038/srep42912

26. Pierce, M., Kahn, J. N., Chiou, J., & Tumer, N. E. (2011). Development of a quantitative RT-PCR assay to examine the kinetics of ribosome depurination by ribosome inactivating proteins using Saccharomyces cerevisiae as a model. *RNA*, *17*(1), 201–210. https://doi.org/10.1261/rna.2375411

27. Li, X.-P., Chiou, J.-C., Remacha, M., Ballesta, J. P. G., & Tumer, N. E. (2009). A two-step binding model proposed for the electrostatic interactions of ricin A chain with ribosomes. *Biochemistry*, *48*(18), 3853–3863. https://doi.org/10.1021/bi802371h

28. Li, X.-P., Grela, P., Krokowski, D., Tchórzewski, M., & Tumer, N. E. (2010). Pentameric Organization of the Ribosomal Stalk Accelerates Recruitment of Ricin A Chain to the Ribosome for Depurination. *Journal of Biological Chemistry*, *285*(53), 41463–41471. https://doi.org/10.1074/jbc.M110.171793

29. Li, X.-P., Kahn, P. C., Kahn, J. N., Grela, P., & Tumer, N. E. (2013). Arginine Residues on the Opposite Side of the Active Site Stimulate the Catalysis of Ribosome Depurination by Ricin A Chain by Interacting with the P-protein Stalk. *Journal of Biological Chemistry*, *288*(42), 30270–30284. https://doi.org/10.1074/jbc.M113.510966

30. Basu, D. (2016). *The role of the A1 subunit in the activity of shiga toxins*. Retrieved from https://rucore.libraries.rutgers.edu/rutgers-lib/51187/